AXL Inhibition Represents a Novel Therapeutic Approach in *BCR-ABL* Negative Myeloproliferative Neoplasms

Antonia Beitzen-Heineke[1,2], Nikolaus Berenbrok[1–4], Jonas Waizenegger[1,3], Sarina Paesler[1,2], Victoria Gensch[1–4], Florian Udonta[1,2], Maria Elena Vargas Delgado[3], Janik Engelmann[1,2], Friederike Hoffmann[5], Philippe Schafhausen[1], Gunhild von Amsberg[1], Kristoffer Riecken[6], Niklas Beumer[3,7,8], Charles D. Imbusch[7], James Lorens[9,10], Thomas Fischer[11], Klaus Pantel[2], Carsten Bokemeyer[1], Isabel Ben-Batalla[1–4], Sonja Loges[1–4]

Correspondence: Sonja Loges (Sonja.Loges@medma.uni-heidelberg.de).

Abstract

BCR-ABL negative myeloproliferative neoplasms (MPNs) consist of essential thrombocythemia, polycythemia vera, and myelofibrosis. The majority of patients harbor the *JAK2*-activating mutation V617F. JAK2 inhibitors were shown to reduce symptom burden and splenomegaly in MPN patients. However, treatment options are limited after failure of JAK2 inhibitors. AXL, a member of the TAM family of receptor tyrosine kinases, mediates survival and therapy resistance of different myeloid cancers including acute myeloid leukemia and chronic myeloid leukemia. We studied the relevance of AXL as a target in MPN using primary patient cells and preclinical disease models. We found that AXL is abundantly activated in MPN cells and that its ligand growth arrest-specific gene 6 is upregulated in MPN patients. Pharmacologic and genetic blockade of AXL impaired viability, decreased proliferation and increased apoptosis of MPN cells. Interestingly, ruxolitinib treatment induced increased phosphorylation of AXL indicating that activation of AXL might mediate resistance to ruxolitinib. Consistently, the AXL inhibitor bemcentinib exerted additive effects with ruxolitinib via impaired STAT3, STAT5, and AKT signaling. Both agents had activity when employed alone and exerted an additive effect on survival and splenomegaly in vivo. Moreover, bemcentinib treatment normalized red blood cell count and hemoglobin levels in vivo. Thus, our data indicate that AXL inhibition represents a novel treatment option in MPN warranting clinical investigation.

[1]*Department for Oncology, Hematology and Bone Marrow Transplantation with the Section Pneumology, Hubertus Wald Tumorzentrum, University Comprehensive Cancer Center Hamburg, Germany*
[2]*Department of Tumor Biology, Center of Experimental Medicine, University Medical Center Hamburg-Eppendorf, Hamburg, Germany*
[3]*Division of Personalized Medical Oncology, German Cancer Research Center (DKFZ), Heidelberg, Germany*
[4]*Department of Personalized Oncology, University Hospital Mannheim, Medical Faculty Mannheim, University of Heidelberg, Mannheim, Germany*
[5]*Practice for Hematology and Oncology Altona, Hamburg, Germany*
[6]*Department of Stem Cell Transplantation, Research Department Cell and Gene Therapy, University Cancer Center Hamburg, University Medical Center Hamburg-Eppendorf, Hamburg, Germany*
[7]*Division of Applied Bioinformatics, German Cancer Research Center (Deutsches Krebsforschungszentrum; DKFZ), Heidelberg, Germany*
[8]*Faculty of Biosciences, Heidelberg University, Heidelberg, Germany*
[9]*Department of Biomedicine, Centre for Cancer Biomarkers, Norwegian Centre of Excellence, University of Bergen, Norway*
[10]*BerGenBio ASA, Bergen, Norway*
[11]*Department of Hematology and Oncology, Medical Center, Otto-von-Guericke University, Magdeburg, Germany*
IBB and SL contributed equally to this article.
Supplemental digital content is available for this article.

Introduction

The *BCR-ABL* negative myeloproliferative neoplasms (MPNs) including polycythemia vera (PV), essential thrombocythemia (ET), and primary myelofibrosis (MF) are characterized by driver mutations with gain-of-function effects on JAK2/STAT signaling.[1] Ruxolitinib has for a long time been the only approved JAK2 inhibitor effective in intermediate and high-risk MF and hydroxyurea-resistant or -intolerant PV. Recently, the approval of fedratinib expanded treatment options for MF patients. However, the effects of JAK2 inhibitors are limited to a reduction of symptom burden and splenomegaly.[2-4] In case of ineligibility for allogeneic hematopoietic cell transplantation or after failure of JAK2 inhibitors, treatment options are scarce. Therefore, new treatment strategies are urgently needed.

AXL belongs to the family of TAM receptor tyrosine kinases and is overexpressed in different solid and hematologic malignancies.[5,6] AXL is activated by its ligand growth arrest-specific gene 6 (GAS6) promoting proliferation, survival, and chemoresistance of different myeloid neoplasms.[7,8] Besides, STAT5 was shown to increase AXL expression via increasing its promotor activity. Thus, aside from GAS6, STAT5-activating stromal cytokines can in principle regulate AXL activity in the bone marrow (BM).[9] Furthermore, activation of AXL through interaction with tyrosine kinases like epidermal growth factor receptor (EGFR) and vascular endothelial growth factor receptor, which activate Src kinases, and with human epidermal growth factor receptor 2 have been described.[10-12] Effects of AXL signaling are mediated by activation of downstream pathways including STAT5 and phosphoinositide 3-kinase signaling pathways, eliciting pro-survival effects.

This pro-survival signaling includes increased expression of antiapoptotic proteins such as B-cell lymphoma 2 (BCL-2) and inhibition of proapoptotic protein such as caspase 3.[5-8,13]

Our previous work in acute myeloid leukemia (AML) indicated that malignant hematopoietic cells induce upregulation of the AXL ligand GAS6 in the BM stroma to foster their growth and to induce therapy resistance. Using the small molecule AXL inhibitor bemcentinib (BGB324) we demonstrated therapeutic potential of AXL blockade in in vivo models of AML.[8] Furthermore, we demonstrated GAS6-AXL signaling in chronic myeloid leukemia (CML) cell lines and patient samples and showed growth inhibition of CML cells by bemcentinib.[7] Bemcentinib represents a well-tolerated, specific AXL inhibitor with clinical activity in AML and is currently under investigation in a phase 2 trial in AML and myelodysplastic syndrome (NCT03824080).[8,14]

Furthermore, AXL expression represents a negative prognostic factor in multiple solid tumors. In non-small-cell lung carcinoma (NSCLC) and melanoma patients, AXL upregulation has been observed in patients with resistance to targeted therapies and in non-responders to immune checkpoint blockade.[15-17] Bemcentinib treatment was shown to overcome resistance to different targeted therapies and to increase chemosensitivity in preclinical models of solid malignancies.[18-23] Currently, bemcentinib is studied in combination with chemotherapy, immunotherapy, or targeted therapies in non-small cell lung cancer (NCT03184571, NCT02922777, NCT02424617), triple negative breast cancer (NCT03184558), pancreatic cancer (NCT03649321), glioblastoma (NCT03965494), malignant mesothelioma (NCT03654833), and melanoma (NCT02872259).[24-26]

Recently, upregulation and activation of AXL has been described in CD34^{+} cells from peripheral blood (PB) of *JAK2V617F* mutated patients and bemcentinib was shown to inhibit colony formation of these cells.[27] Based on these data and on the important role of AXL in malignant hematopoiesis, we studied the relevance of AXL in *BCR-ABL* negative MPN in vivo. Thereby we found that bemcentinib has therapeutic potential both alone and in combination with ruxolitinib.

Materials and methods

Animals

Six- to 8-week-old NOD.C-Prkdc[scid]Il2rg[tm1Wjl]/SzJ (NSG) mice were used. All animal experiments were carried out in concordance with the institutional guidelines for the welfare of animals in experimental neoplasia and were approved by the local licensing authority (Behörde für Soziales, Gesundheit, Familie, Verbraucherschutz; Amt für Gesundheit und Verbraucherschutz, project number G93/17). Housing, breeding, and experiments were performed under a 12 hours light—12 hours dark cycle and standard laboratory conditions (22 ± 1°C, 55% humidity, food, and water ad libitum, and 150–400 lx light intensity during the light phase).

Patient samples

AXL expression levels were analyzed in BM mononuclear cells (BMMNCs) from patients with untreated *BCR-ABL* negative MPN from the University Hospital Hamburg-Eppendorf. MNCs were isolated from PB and BM using Ficoll-Paque density centrifugation. This analysis was carried out with approval of the local medical ethics committee (approval number MC-220/13). Additional plasma samples were provided by the Cambridge Blood and Stem Cell Biobank. All studies with human samples were carried out in accordance with the Declaration of Helsinki.

Cell culture

UKE-1 cells (kindly provided by Walter Fiedler, Hamburg, Germany) were cultured in Iscove's modified dulbecco's medium supplemented with 10% fetal bovine serum (FBS), 10% horse serum, 1% penicillin/streptomycin (P/S), and 1 μM hydrocortisone. HEL cells (german collection of microorganisms and cell cultures [DMSZ]) were cultured in Roswell Park Memorial Institute Medium (RPMI)-1640 medium (all cell culture reagents purchased from Invitrogen, Darmstadt, Germany) supplemented with 20% FBS, 1% P/S, and 1% L-glutamine. SET-2 (DMSZ) and Baf3 cells expressing erythropoietin receptor (BaF3-EpoR)-*JAK2V617F* cells (kindly provided by Thomas Fischer, Magdeburg, Germany) were cultured in RPMI-1640 medium, supplemented with 10% FBS, 1% P/S, and 1% L-glutamine. For BaF3-EpoR-*JAK2V617F* cells, 50 nM 4-(2-hydroxyethyl)-1-piperazineethanesulfonic acid, 5 mM sodium pyruvate, and 0.6% non-essential amino acids were added to culture medium. Human cell lines were authenticated.

Treatments and in vitro assays

Experiments were performed in serum-deprived medium (0.1% FBS) and normal medium conditions, as indicated in the figure legends. Bemcentinib (gift from BerGenBio), ruxolitinib, and CHZ868 (both MedChem Express) were dissolved in dimethylsulfoxide and used in different concentrations as indicated in the figure legends. To assess cell viability, 4×10^4 cells/well were seeded in 96 well plates and treated with the indicated drug and GAS6 concentrations, respectively. After 48 hours, cell numbers were assessed by water soluble tetrazolium salts assay (Roche Applied Science, Mannheim, Germany). To assess proliferation and apoptosis, 2×10^5 cells/well were seeded in 24 well plates and treated with the indicated concentration of bemcentinib. Proliferation levels were measured by flow cytometry using bromodeoxyuridine/5-bromo-2′-deoxyuridine (BrdU) incorporation assays (Becton and Dickinson bromodeoxyuridine/5-bromo-2′-deoxyuridine ([BD]). Apoptosis levels were measured by flow cytometry using 7-aminoactinomycin D (7-AAD) staining (to exclude dead cells) and Annexin V-FITC. Events were captured using BD fluorescence- activated cell sorting Calibur.

Enzyme-linked immunosorbent assay

Human GAS6 levels were determined in PB and BM plasma using enzyme-linked immunosorbent assay kits according to the manufacturer's instructions (R&D Systems).

Colony-forming assay

Growth potential of hematopoietic progenitor cells from PB in the presence of bemcentinib was determined by colony-forming cell assay. For that, 4×10^5 PB mononuclear cells (PBMNCs) were aliquoted in triplicate in semisolid culture medium (Methylcellulose H4034; Stem Cell Technologies) and cultured for 14 days and colonies were scored by light microscope.

Cloning of lentiviral gene ontology vectors and production of lentiviral particles

Cloning of lentiviral gene ontology vectors (LeGO) for silencing human *AXL* was performed as previously described[28] (for detailed protocols and vector maps refer to http://www.lentigo-vectors.de). For silencing *AXL* pLKO.1 vector containing short hairpin ribonucleic acid (shRNA) *AXL* sequence 5′-ccggcgaaatcctctatgtcaacatctcgagatgttgacatagaggatttcgtttt-3′ was purchased from Sigma MISSION. The complete sequence of shRNA *AXL*, including the U6 promotor, was cloned in a

LeGO-Cerulean-Blasticidin vector. PspOMI and XhoI (New England Biolabs) enzymes were used to cut the vector backbone, NotI and SalI producing compatible overhangs were used to cut the polymerase chain reaction (PCR) fragment. Sequences of primers used for PCR amplification to enrich sequence from pLKO.1 vector are as follows, forward primer: 5′-acggtatcgat-cacgagactagcctcgagc-3′ and reverse primer: 5′-tactgccatttgt-gtcgacgtcgagaattc-3′. Knockdown of *AXL* was confirmed by quantitative PCR (qPCR) and western blotting. After transduction of SET-2 cell line with fluorochrome-expressing lentiviral vectors mediating *AXL* knockdown, percentage of knockdown cells was determined using flow cytometry. Only cells with a minimum of 70% knockdown as measured by qPCR compared with controls were used for experiments.

Western blot analysis

To assess the levels of protein expression using western blotting, cells or tissue were lysed in RIPA buffer with protease and phosphatase inhibitors. Western blotting was performed as described.[8] The phosphorylated protein kinase B (pAKT), AKT, p-p44/42 mitogen-activated protein kinase (MAPK) (phosphorylated extracellular-signal-regulated kinase 1/2), p44/42 MAPK (extracellular-signal-regulated kinase 1/2), phosphorylated signal transducer and activator of transcription (pSTAT)5, STAT5, STAT5A, STAT5B, pSTAT3, STAT3, BCL-2, cleaved caspase 3 (CC3), Lamin B1, and X-linked inhibitor of apoptosis protein antibodies were purchased from Cell Signaling (distributed through New England Biolabs GmbH). β-Actin and β-Tubulin antibodies were purchased from Santa Cruz Biotechnology, α-Tubulin antibody from Sigma-Aldrich. Phosphorylated AXL (pAXL) antibody (Y779), which detects human and mouse AXL when phosphorylated at Y779, a well conserved motif in humans (according to phosphosite.org), was purchased from R&D Systems. The AXL antibody was a gift from Björn Dahlbäck, Malmö, Sweden. For detailed information on the antibodies please refer to Supplemental Table 2 (http://links.lww.com/HS/A188). The NE-PER kit (ThermoFisher Scientific) was used for extraction of nuclear and cytoplasmic protein according to the manufacturer's instructions.

Mouse models of *JAK2V617F*-driven disease

For the SET-2 xenograft model, 10×10^6 cells in PBS were injected subcutaneously into the flank of NSG mice. Mice were randomized and treated twice daily with vehicle (0.5% hydroxypropyl Methylcellulose/0.1% Tween 80), or 50 mg/kg bemcentinib by oral gavage. Mice were sacrificed when the first tumor reached a size of 1500 mm³. Tumors were weighed and divided to obtain pieces for embedding in paraffin for further immunohistochemistry analysis and fresh tissue was frozen for protein extracts for western blot analysis. For the systemic model, 2.5×10^2 BaF3-EpoR-*JAK2V617F* cells were injected intravenously into 6–8-week-old NSG mice. The next day, treatment with vehicle (bemcentinib vehicle as described above, ruxolitinib vehicle: 5% dimethylacetamide, 0.5% methocellulose) or 50 mg/kg bemcentinib, 50 mg/kg ruxolitinib or combination of bemcentinib and ruxolitinib was initiated via oral gavage twice daily. Hematologic parameters were measured using a Sysmex KX-21N. Ruxolitinib phosphate, for in vivo experiments, was provided by Novartis Pharma AG.

Immunohistochemistry of phospho-histone H3

Tumors were fixed overnight in 1% paraformaldehyde at 4°C and embedded in paraffin. Tumor sections were stained with a primary antibody against phospho-histone H3 (pHH3) as a mitosis-specific marker overnight at 4°C (1:100, from Cell Signaling Technology Inc., Danvers, MA). Sections were developed with ZytoChem horseradish peroxidase Kit, Broad spectrum (Zytomed Systems, Berlin, Germany) as described in the manual and counterstained with hematoxylin. Image analysis was performed using AxioVision imaging software (Carl Zeiss Microscopy, Scope.A1). Automated counting of immunostained cells in the tumor stroma was performed in 10 to 12 fields of each tumor section at ×10 magnification using ImageJ 1.8.0 software. pHH3 positive cells were calculated as the number of counted pHH3+ cells per square millimeter of analyzed tumor tissue. Areas of necrosis were excluded from all analysis.

Statistical analysis

Data represent mean ± SEM of representative experiments and statistical significance was calculated by Student's t-test, unless otherwise stated. To study dependence of numerical-dependent parameters of n > 2 categorical variables, ANOVA was used where indicated. Survival analysis was carried out using the Kaplan-Meier method (log-rank test). All statistical analyses were performed using GraphPad Prism 5 software.

Results

Primary MPN cells show high levels of AXL expression

Upregulation and activation of AXL in MPN was first described by Pearson et al[27] and our first aim was to further confirm that AXL could represent a target in MPN. Therefore, we investigated AXL protein expression by BMMNC of untreated *BCR-ABL* negative MPN patients compared with healthy donors by western blot analyses. We found high levels of phosphorylated AXL in patient samples (n = 6, for patient characteristics see Supplemental Table 1, http://links.lww.com/HS/A188) compared with healthy donors (n = 3, *P < 0.05, Figure 1A), demonstrating increased signaling receptor activity in MPN patients. Furthermore, GAS6 protein levels in BM plasma of MPN patients were significantly increased compared with healthy donors (n = 11/22, *P < 0.05, Figure 1B). GAS6 quantification in PB plasma of patients and healthy donors did not detect differences in GAS6 in the whole cohort (n = 30/14, Figure 1C). However, subgroup analysis of MF patients showed significantly increased levels of GAS6 compared with healthy donors (n = 13/14, *P < 0.05, Figure 1D). These data indicate activation of the GAS6-AXL pathway in MPN patients.

Pharmacological inhibition of AXL decreases colony-forming potential of primary MPN cells

To investigate the biological effects and therapeutic potential of AXL inhibition in MPN cells, the small molecule AXL kinase inhibitor bemcentinib was utilized. PBMNCs were isolated from MPN patients or healthy donors (n = 5/5) and colony assays were performed in absence or presence of bemcentinib. Quantification of growth of erythroid progenitor cells (burst forming unit-erythroid [BFU-E]), multipotential granulocyte, erythroid, macrophage, and megakaryocyte progenitor cells (colony forming unit - granulocyte, erythrocyte, monocyte, megakaryocyte), and granulocyte-macrophage progenitor cells (colony forming unit – granulocyte, monocyte [CFU-GM]) demonstrated that bemcentinib reduced the number of BFU-E but not CFU-GEMM or CFU-GM colonies at day 14. This reduction of BFU-E growth was higher in samples from MPN patients compared with healthy donors indicating a therapeutic
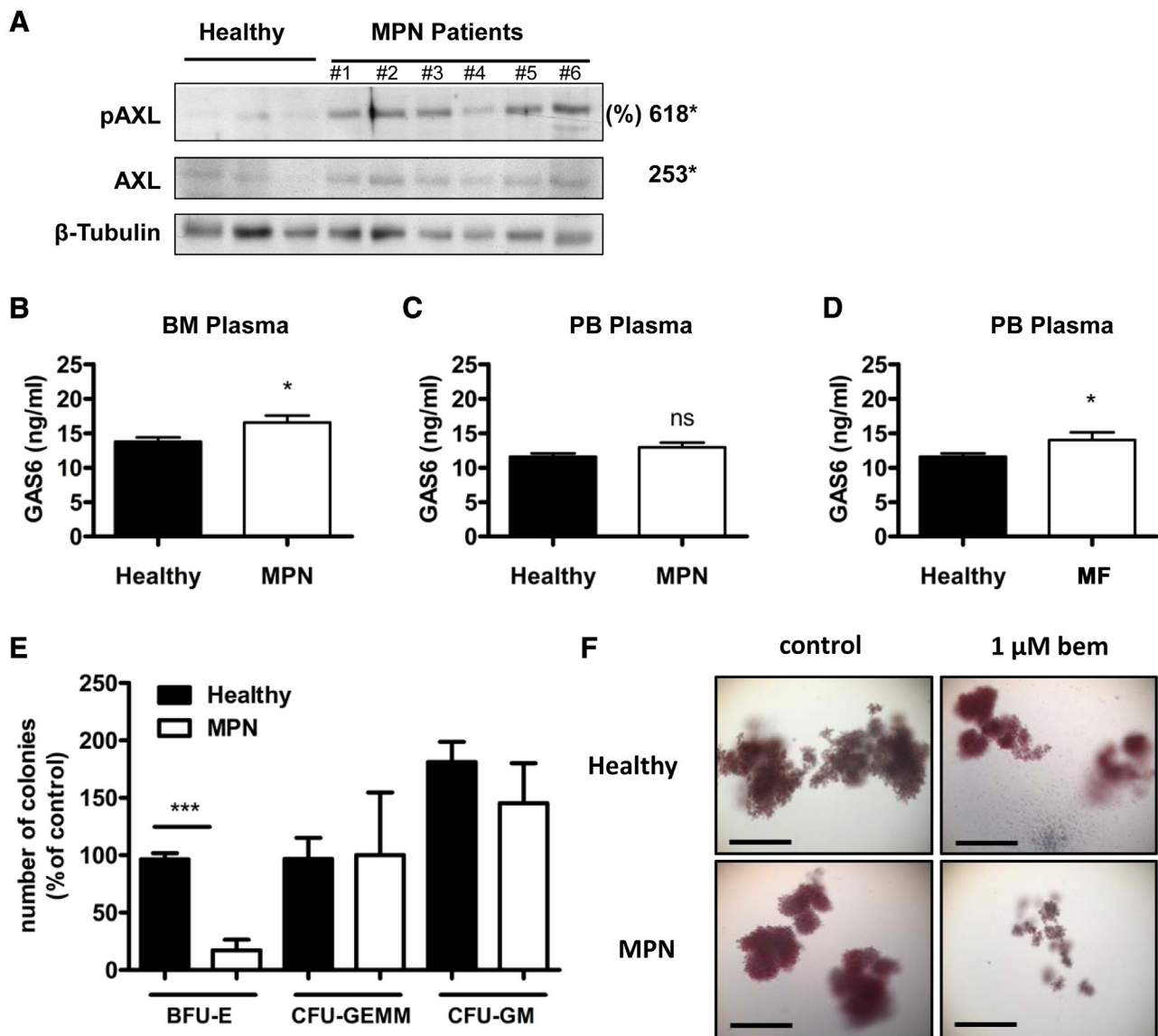
Figure 1. AXL represents a target in MPN patients. Western blot analysis of phosphorylated and total AXL expression was performed in BMMNCs from untreated MPN patients compared with healthy donor samples (n = 6/3). β-Tubulin was used as loading control. Densitometric quantification of (protein expression/β-Tubulin expression) was normalized to healthy samples and represented as percentage (A). GAS6 protein levels were measured by ELISA in BM plasma from MPN patients (n = 11) compared with healthy controls (n = 22) (B) and in PB plasma from MPN patients (n = 30) and healthy controls (n = 14) (C). Subgroup analysis of GAS6 levels in PB plasma from MF patients (n = 13) compared with healthy donors was performed (D). Human peripheral blood mononuclear cells were cultured in semisolid medium with bemcentinib (bem, 1 μM) and number of CFUs was counted after 14 d. Percentage of colony number was normalized to control treatment of the same healthy donor or patient. Quantification of colonies BFU-E, CFU-GEMM, and CFU-GM is shown. The mean number of colonies counted in all control-treated samples was 28 ± 5 (mean ± SEM) (E). Representative pictures of BFU-E from patient and healthy control, bar represents 200 μm (F) (*$P < 0.05$, ***$P < 0.001$, ns not significant). BFU-E = burst forming unit-erythroid; BM = bone marrow; BMMNC = bone marrow mononuclear cell; CFU = colony-forming unit; CFU-GEMM = colony forming unit - granulocyte, erythrocyte, monocyte, megakaryocyte; CFU-GM = colony forming unit – granulocyte, monocyte; GAS6 = growth arrest-specific gene 6; MF = myelofibrosis; MPN = myeloproliferative neoplasm; ns = not significant; pAXL = phosphorylated AXL; PB = peripheral blood.

window for the drug (83% versus 4%, n = 5/5, ***$P < 0.001$, Figure 1E–F).

Pharmacological inhibition of AXL decreases viability of JAK2-V617F⁺ cells

In a next step, we evaluated AXL expression in different MPN cell lines harboring the *JAK2V617F* mutation, such as UKE-1, HEL, SET-2, and BaF3-EpoR-*JAK2V617F* cells.[29] Immunoblotting revealed presence of AXL expression in SET-2 and BaF3-EpoR-*JAK2V617F* cells (Figure 2A). Therefore, we utilized SET-2 and BaF3-EpoR-*JAK2V617F* as cellular models

for AXL⁺ MPN in further experiments while UKE-1 and HEL cells represent negative controls for specificity of AXL-targeting.

Interestingly, AXL phosphorylation in SET-2 cells was augmented in serum-deprived medium indicating increased activation of AXL in challenging conditions (Figure 2B). Furthermore, after treatment of SET-2 cells with ruxolitinib, increased AXL phosphorylation was detected, suggesting that AXL activation might constitute a signaling pathway bypassing the effects of JAK2 blockade by ruxolitinib (Figure 2C). Thus, concomitant inhibition of AXL and JAK2 could potentially exert additive therapeutic effects. In contrast to the effect seen with ruxolitinib, we observed a slight decrease of AXL phosphorylation after treatment with a type II JAK2 inhibitor (CHZ868), which does not
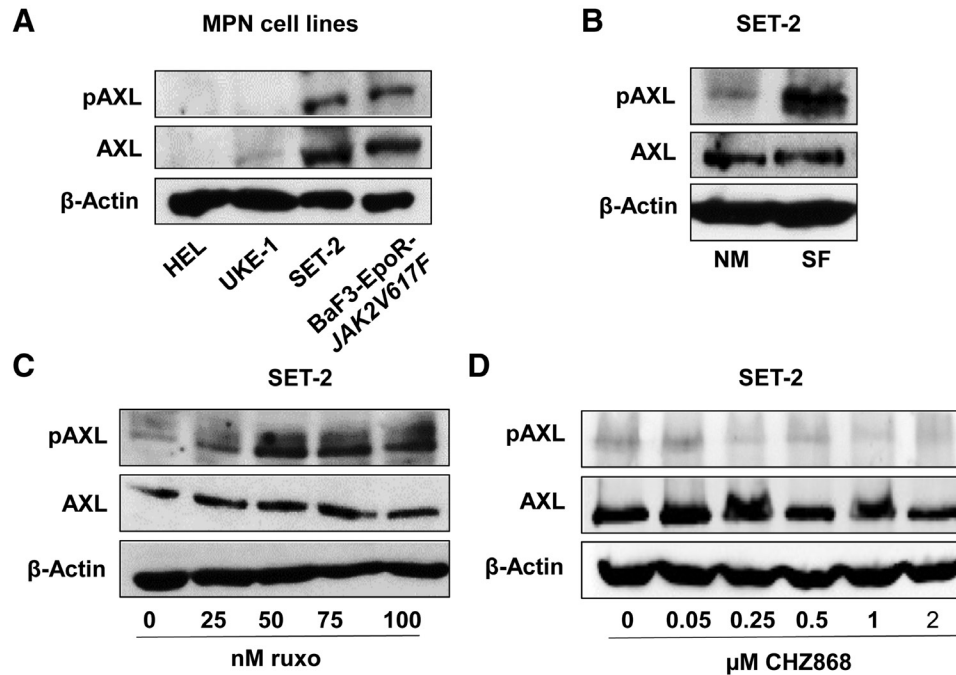
Figure 2. AXL activation in MPN cell lines. Western blot analysis of pAXL and total AXL expression was performed in human *JAK2V617F* mutated HEL, UKE-1, SET-2, and murine BaF3-EpoR-*JAK2V617F* cells (A). Western blot analysis of pAXL in SET-2 cells is shown after 1 h of culturing the cells in NM (containing 10% FBS) compared with culturing in serum-deprived conditions (SF, containing 0.1% FBS) (B). SET-2 cells were cultured for 1 h in SF medium with indicated concentrations of ruxolitinib (ruxo) (C) or CHZ868 (D) followed by western blot analysis of pAXL and total AXL expression (C and D). β-Actin was used as loading control. FBS = fetal bovine serum; MPN = myeloproliferative neoplasm; NM = normal medium; pAXL = phosphorylated AXL; SF = serum free medium.

cause hyperphosphorylation of JAK2 (Figure 2D). Furthermore, co-immunoprecipitation studies revealed that anti-JAK2 antibody could pull down AXL (Supplemental Figure 1, http://links.lww.com/HS/A188) indicating physical interaction of JAK2 and AXL.

To investigate the therapeutic potential of AXL in MPN cells, AXL expressing MPN cell lines were treated with bemcentinib. Consistent to the observations in primary MPN cells, in SET-2 and BaF3-EpoR-*JAK2V617F* cells, a dose-dependent reduction in cell viability was observed upon treatment with bemcentinib (Figure 3A and B). Notably, the half maximal inhibitory concentration (IC_{50}) levels were in the range of bemcentinib plasma levels achieved by the recommended phase 2 dose in AML patients.[30] In contrast, viability of AXL⁻ cell lines UKE-1 and HEL was not reduced upon treatment with bemcentinib indicating specificity of the drug for AXL expressing MPN cells (Supplemental Figure 2A and B, http://links.lww.com/HS/A188). Furthermore, treatment with GAS6 showed increased viability in AXL expressing cell lines but not for AXL⁻ UKE-1 and HEL cells (Supplemental Figure 3A–D, http://links.lww.com/HS/A188). Subsequently, we wanted to elucidate whether reduced cell viability was caused by augmented apoptosis and/or diminished proliferation ratio. For both AXL⁺ cell lines, BrdU assays revealed a dose dependent decrease in the rate of proliferating cells in the presence of bemcentinib (Figure 3C and D) and increased apoptosis rates in Annexin V⁺ assays (Figure 3E and F). Serum-deprived conditions were used in order to mimic challenging conditions and to prevent interference with GAS6 that is a component in FBS. However, the observed effects of bemcentinib on SET-2 and BaF3-EpoR-*JAK2V617F* are not dependent on serum starvation and were observed in normal medium conditions as well (Supplemental Figure 4, http://links.lww.com/HS/A188). These results showed that AXL blockade by bemcentinib leads to induction of apoptosis and reduction of proliferation in MPN cells.

To further investigate the mechanisms by which bemcentinib exerts its biological effects, MPN cells were incubated with different concentrations of bemcentinib followed by western blot analyses. Analysis of signal transduction intermediates revealed a dose-dependent reduction of pAXL levels consistent with on-target activity of bemcentinib. Furthermore, bemcentinib reduced STAT5 phosphorylation in SET-2 cells and AKT phosphorylation in BaF3-EpoR-*JAK2V617F* cells (Figure 4A and B), which represent important signaling pathways promoting proliferation and survival. In addition, we performed cytoplasmatic and nuclear protein extraction in SET-2 cells and observed significant reduction of pSTAT5 levels in the cytoplasm but not in the nucleus upon bemcentinib treatment. Likewise, STAT5A and STAT5B were mostly located in the cytoplasm and levels were not affected by bemcentinib treatment (Figure 4C). Investigation of important regulators of apoptosis[31-33] revealed that bemcentinib treatment resulted in increased CC3 levels (Figure 4D).

These data were corroborated by lentiviral shRNA-mediated knockdown of *AXL* (shAXL) in SET-2 cells (Figure 5). Silencing of *AXL* in SET-2 cells showed significantly reduced cellular viability compared with control transduced cells (Figure 5A). Concomitantly, proliferation of shAXL transduced cells was significantly inhibited (Figure 5B) and the apoptosis rate was increased compared with control transduced SET-2 cells (Figure 5C). Knockdown of *AXL* effectively reduced expression of total AXL and AXL activity (Figure 5D). Downstream signaling of STAT5 and STAT3 was reduced in *AXL* knockdown cells compared with control. Furthermore, increased levels of CC3 confirmed increased apoptosis of shAXL SET-2 cells compared with control-transduced cells (Figure 5D). Overexpression of AXL by lentiviral gene transfer increased sensitivity of SET-2 cells to bemcentinib compared with control-transduced cells, indicating that the inhibitory effects of bemcentinib in SET-2 cells are mediated via inhibition of AXL signaling (Supplemental
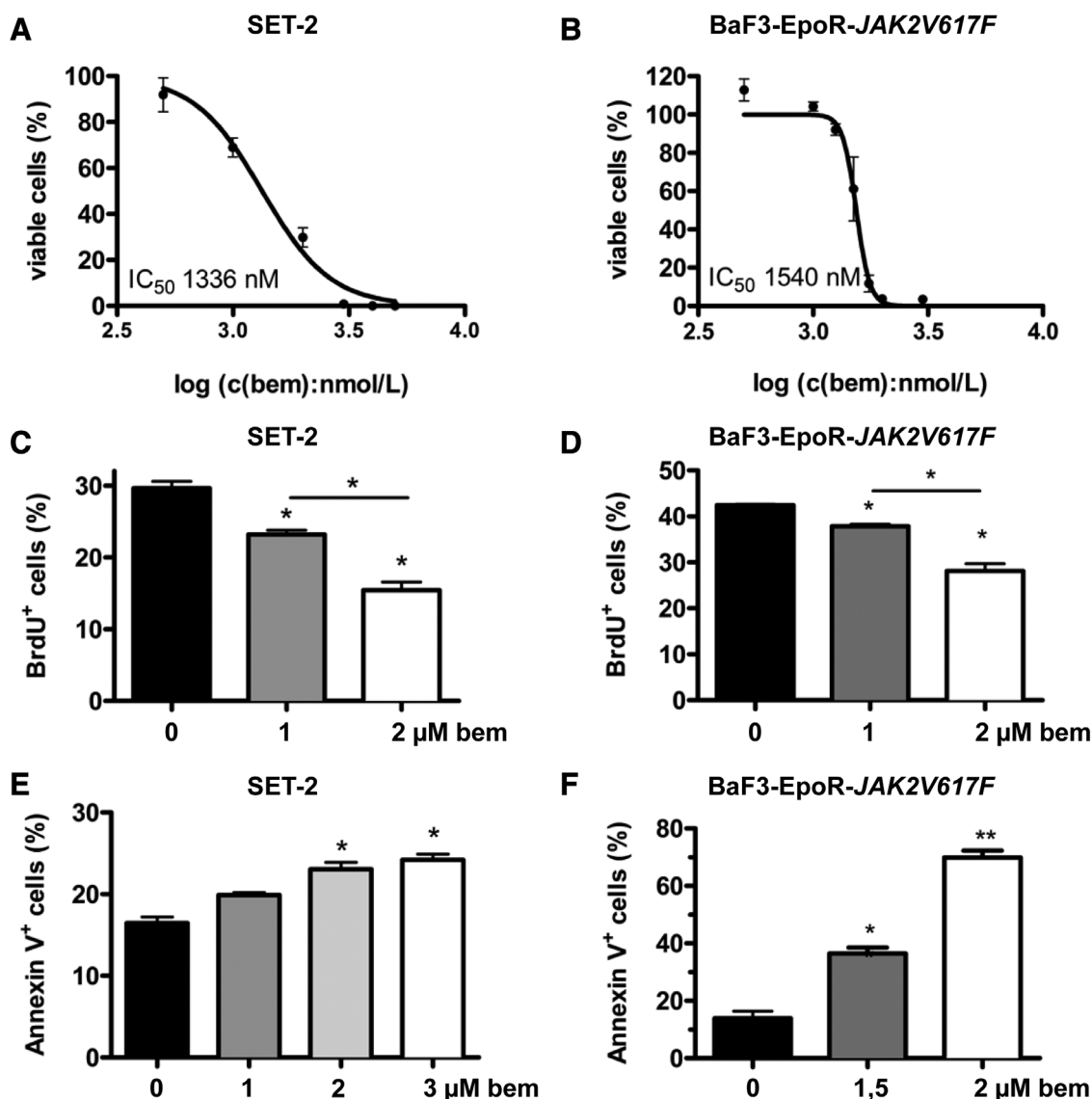
Figure 3. Bemcentinib (bem) inhibits proliferation and induces apoptosis in AXL $^+$ MPN cell lines. Assessment of half maximal inhibitory concentration (IC_{50}) for bem. Treatments were performed with increasing concentrations (0, 0.5, 1, 2, 3, 4, 5 µmol/L, n = 3) of bem (log10 scale) for 48 h with human SET-2 cells (A) and murine BaF3-EpPoR-*JAK2V617F* cells (B). WST-1 cell viability assays were performed. Percentage of viable cells was normalized to control-treated cells (A and B). SET-2 cells (C) and BaF3-EpoR-*JAK2V617F* cells (D) were incubated with bem for 24 h (0, 1, 2 µM bem, n = 2) and FACS quantification of proliferation (BrdU staining) was performed (C and D). FACS quantification of apoptosis (Annexin V staining) was performed after incubating SET-2 cells (0, 1, 2, 3 µM bem, 12 h incubation, n = 2) (E) and BaF3-EpoR-*JAK2V617F* cells (0, 1.5, 2 µM bem, 24 h incubation, n = 2) (F) with bem (E and F). Experiments were performed in serum-deprived conditions (*$P < 0.05$, **$P < 0.01$). BrdU = bromodeoxyuridine/5-bromo-2'-deoxyuridine; FACS = fluorescence-activated cell sorting; MPN = myeloproliferative neoplasm; WST-1 = water soluble tetrazolium salts.

Figure 5, http://links.lww.com/HS/A188). Altogether, these experiments demonstrated that AXL signaling is a driver of survival and proliferation in MPN and its inhibition represents a potential therapeutic target in this disease.

Blockade of AXL exerts additive therapeutic effects with ruxolitinib in *JAK2V617F* mutated cell lines

Next, we sought to elucidate whether concomitant inhibition of AXL and JAK2 has additive effects on the viability of MPN cells. Therefore, viability assays were performed combining different doses of bemcentinib und ruxolitinib. Interestingly, concomitant inhibition of AXL and JAK2 exerted additive inhibitory effects on viability of SET-2 and BaF3-EpoR-*JAK2V617F* cells in serum-deprived and normal medium conditions (Figure 6A–D

and Supplemental Figure 6, http://links.lww.com/HS/A188). To unravel the underlying signaling pathways, key downstream pathways activated by AXL- and JAK2-signaling were investigated by western blot. In SET-2 cells we found an additive inhibitory effect on pSTAT5 and pSTAT3 (Figure 6E). In BaF3-EpoR-*JAK2V617F* cells, we identified additive inhibitory effects of both drugs on pAKT levels (Figure 6F). Thus, the blockade of AXL signaling not only holds potential to inhibit MPN cells, but also increases sensitivity towards ruxolitinib.

Bemcentinib reduces tumor growth in vivo

Encouraged by the in vitro data indicating therapeutic potential of Axl inhibition in *BCR-ABL* negative MPN cells, we decided to investigate the effects of bemcentinib in vivo. For this purpose, we
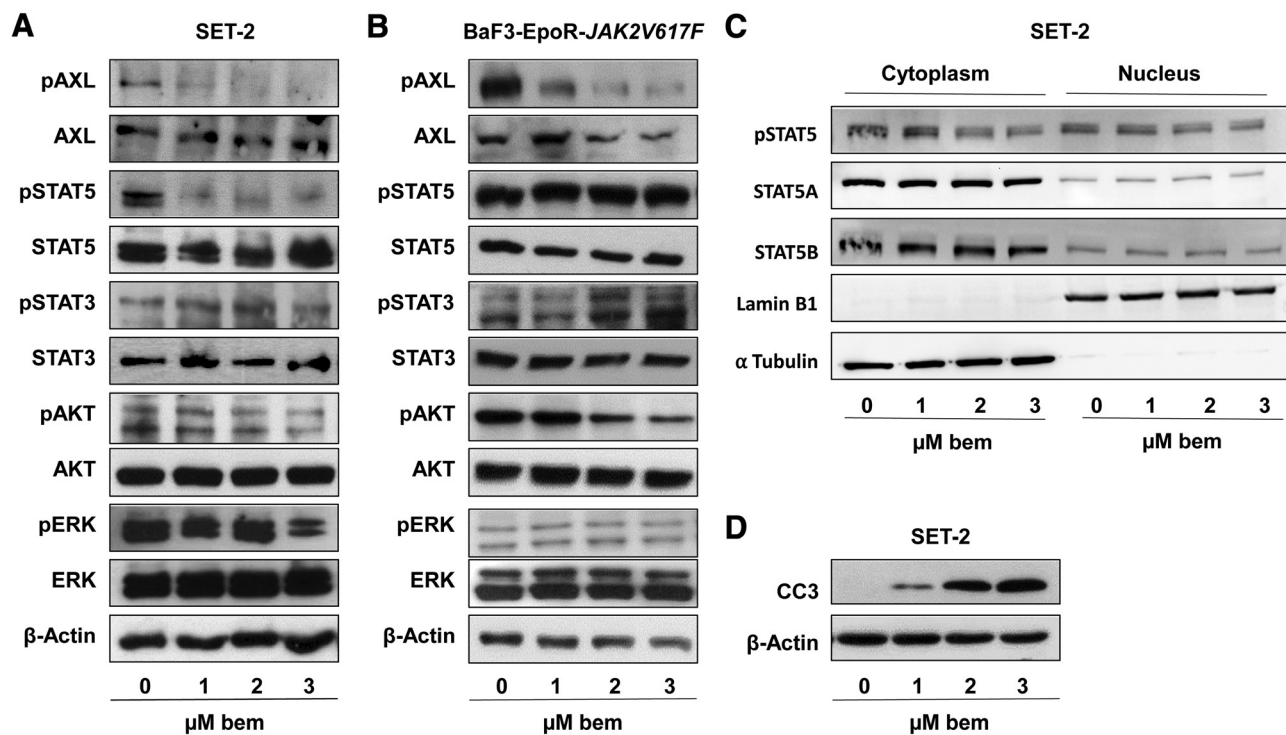
Figure 4. Bemcentinib (bem) inhibits AXL signaling in MPN cell lines. Western blot analysis of pAXL and downstream pathways after incubation with different concentrations of bem in SET-2 cells (time of incubation 1 h) (A) and BaF3-EpoR-*JAK2V617F* cells (time of incubation 3 h) (B) are shown. β-Actin was used as loading control (A and B). After incubation of SET-2 cells with indicated concentrations of bem (time of incubation 1 h) cytoplasmatic and nuclear protein extraction was performed followed by western blot. α-Tubulin and Lamin B1 were used as loading controls for cytoplasmic and nuclear protein, respectively (C). Western blot analysis of CC3 was performed after 24 h of incubation with indicated concentrations of bem in SET-2 cells (D). Treatments were performed in serum-deprived conditions. CC3 = cleaved caspase 3; MPN = myeloproliferative neoplasm; pAKT = phosphorylated AKT; pAXL = phosphorylated AXL; pERK = phosphorylated ERK; pSTAT = phosphorylated STAT.

utilized a xenograft mouse model, in which human SET-2 cells were inoculated subcutaneously into NOD severe combined immunodeficiency gamma (NSG) mice.[34] The animals were randomized into placebo and bemcentinib (50 mg/kg) treatment groups after the tumors reached a size of 100 mm³. We found a 60% inhibition of tumor growth in mice treated with bemcentinib compared with control-treated mice (placebo: 1432 ± 403 mm³, bemcentinib: 632 ± 229 mm³, *P < 0.05, Figure 7A and B). Thus, AXL inhibition significantly reduced tumor growth of MPN cells in vivo. To further investigate the effects of bemcentinib on SET-2 tumor growth, histomorphometric analysis of pHH3 revealed reduced proliferation of SET-2 cells in bemcentinib-treated tumors compared with control (Figure 7C and D), as observed in in vitro experiments. Immunoblotting of different apoptosis markers revealed increased proapoptotic and decreased antiapoptotic markers in bemcentinib-treated tumor tissue compared with control, corroborating our in vitro data (n = 8/8, *P < 0.05, **P < 0.01, Figure 7E).

Bemcentinib prolongs survival and reduces spleen size in MPN in vivo

Next, we tested the efficacy of bemcentinib and concomitant AXL and JAK2 blockade in a systemic mouse model. For this in vivo model of *JAK2V617F* driven disease, BaF3-EpoR-*JAK2V617F* cells were intravenously injected into NSG mice as described previously.[29] One day after injection, mice were randomized into 4 groups and treated with vehicle, bemcentinib, ruxolitinib, or bemcentinib plus ruxolitinib. Combined treatment with both drugs resulted in prolonged overall survival compared with single drug-treated mice (Figure 8A).

To address toxicity issues and pharmacologic impact on organ infiltration, a cohort of mice was sacrificed on day 18 (n = 6/6/7/7). Vehicle-treated mice presented with splenomegaly,

which was significantly reduced in bemcentinib- as well as ruxolitinib-treated mice compared with vehicle-treated mice. More importantly, combined treatment with bemcentinib and ruxolitinib resulted in a significant higher decrease in splenomegaly compared with ruxolitinib alone (Figure 8B and C). Thus, these results confirm the additive effects of combined JAK2 and AXL blockade as seen in the survival analysis and in in vitro experiments.

Interestingly, blood counts revealed higher levels of red blood cells (RBCs) and hemoglobin in bemcentinib-treated mice in the single drug-treated mice as well as in the combination group, suggesting that AXL inhibition has positive effects on erythropoiesis and can improve anemia (Figure 8D and E). Importantly, RBC and hemoglobin levels in bemcentinib-treated mice were comparable to those of healthy NSG mice.[35] Moreover, mean cellular volume (MCV) and mean cellular hemoglobin (MCH) shifted towards normal levels in bemcentinib-treated mice while no significant change in hematocrit was observed (Figure 8F and Supplemental Figure 7A and B, http://links. lww.com/HS/A188). No changes in white blood cell count and platelet count were observed in neither bemcentinib- nor combo-treated mice (Supplemental Figure 7C and D, http://links. lww.com/HS/A188). Altogether, the differential blood counts show that combined treatment with bemcentinib and ruxolitinib does not cause cytopenia, instead the addition of bemcentinib in the combo group improved the RBC and hemoglobin levels compared with ruxolitinib single drug-treated mice.

Concerning toxicity, no changes in body weight or body condition score were observed between treatment groups (Supplemental Figure 8, http://links.lww.com/HS/A188). Also, no changes in gross organ- or stool appearance were evident. Also, transaminases (Supplemental Figure 9, http://links.lww. com/HS/A188) and creatinine levels were not increased above
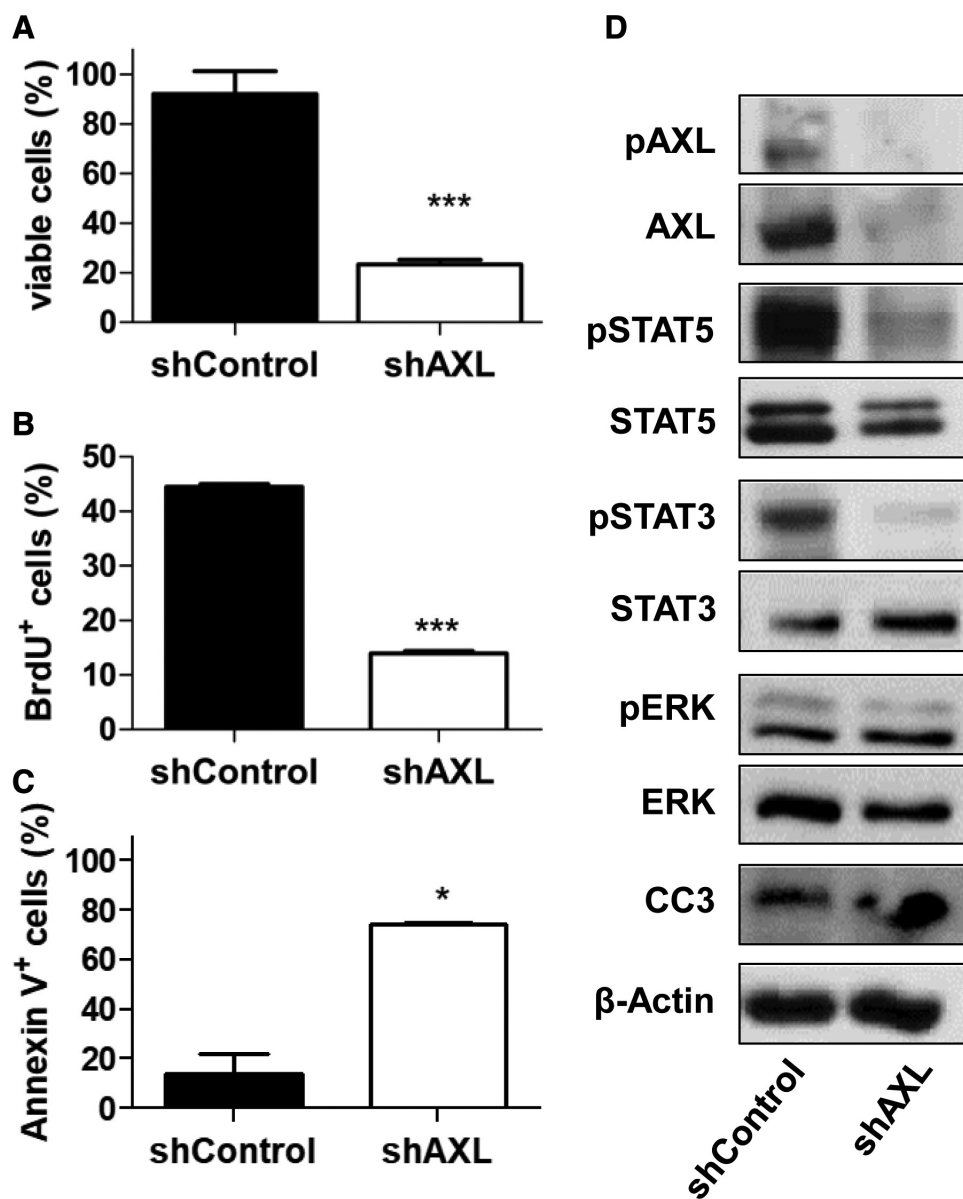
Figure 5. Genetic blockade of AXL inhibits growth of SET-2 cells. *AXL* was silenced in SET-2 cells using shRNA. Cell viability was assessed using WST-1 assay (n = 3) (A), proliferation was quantified by BrdU incorporation assay (n = 2) (B), and rate of apoptosis was measured by FACS after Annexin V staining (n = 2) (C) in shAXL compared with control transduced (shControl) SET-2 cells (A–C) (*P < 0.05, ***P < 0.001). Western blot analysis of pAXL, AXL and downstream signaling pathways was performed in shAXL and shControl SET-2 cells. β-Actin was used as loading control (D). BrdU = bromodeoxyuridine/5-bromo-2'-deoxyuridine; CC3 = cleaved caspase 3; FACS = fluorescence- activated cell sorting; pAXL = phosphorylated AXL; pERK = phosphorylated ERK; pSTAT = phosphorylated STAT; shRNA = short hairpin ribonucleic acid; WST-1 = water soluble tetrazolium salts.

normal excluding relevant hepato- or renal toxicity of the drug combination (data not shown).

Our data show that blockade of AXL has therapeutic potential in vivo and that simultaneous AXL and JAK2 blockade exert additive effects on overall survival, reduce splenomegaly and ameliorate MPN-induced anemia in an aggressive systemic MPN model.

Discussion

The JAK2-inhibitor ruxolitinib has improved treatment for MF and PV significantly. However, therapeutic options are still limited in the case of inadequate response and after ruxolitinib failure. Therefore, there is an urgent need for the identification of novel therapies to expand treatment options for MPN patients.[36]

By analyzing primary patient samples and different models of *JAK2V617F* driven disease, our study demonstrates that AXL represents a novel therapeutic target in *BCR-ABL* negative MPN. To the best of our knowledge, this study is the first to show high levels of activated AXL in untreated MPN patients compared with healthy donors. This finding confirms previously published data by Pearson et al[27] describing upregulation and activation of AXL in primary cells isolated from JAK2-mutated pre-treated MPN patients. We furthermore showed that genetic knockdown, as well as pharmacologic blockade of AXL using bemcentinib, inhibit proliferation and induce apoptosis of *JAK2V617F+* cell lines.
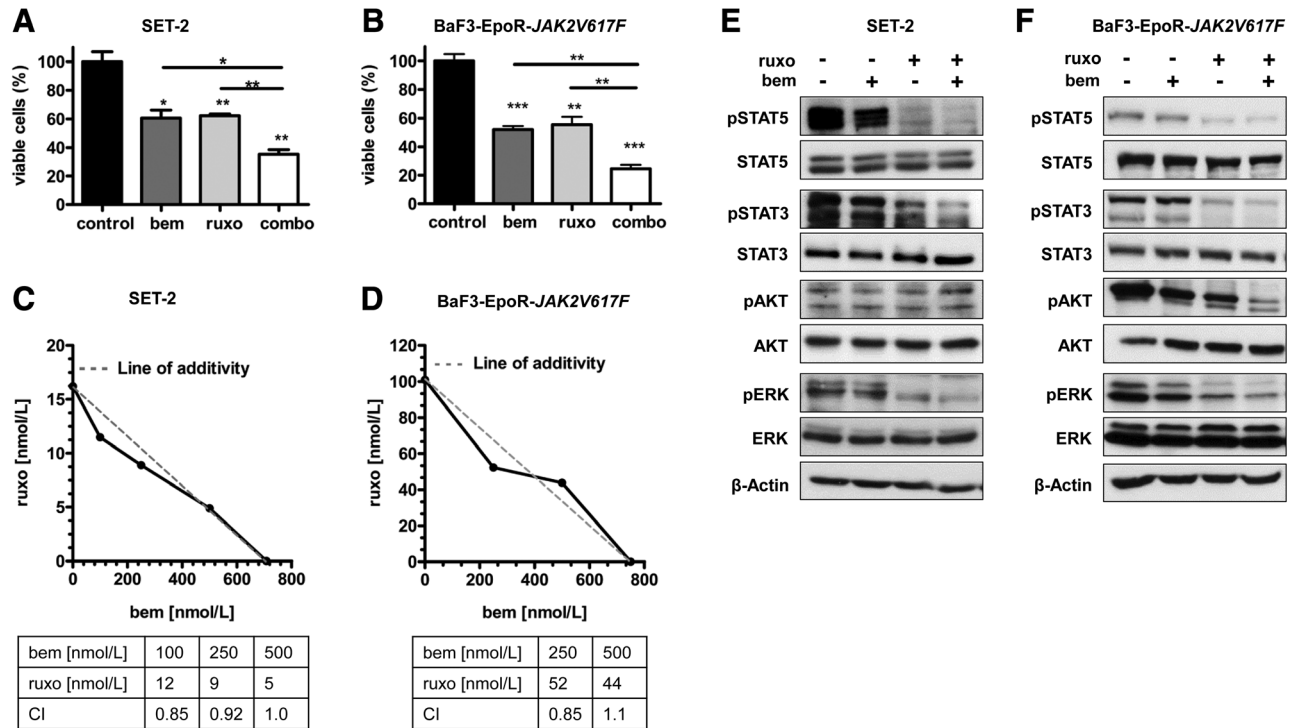
Figure 6. Bemcentinib (bem) and ruxolitinib (ruxo) exert additive inhibitory effects in vitro. SET-2 and BaF3-EpoR-*JAK2V617F* cells were treated with different concentrations of bem and ruxo as single treatment or in combination for 48h in serum-deprived conditions, and cell viability was measured by WST-1 assay. Percentage of viable cells was normalized to control-treated cells (n = 3, *P < 0.05, **P < 0.01, ***P < 0.001). For SET-2 cells, combination of 500nM bem and 10nM ruxo is shown (A). For BaF3-EpoR-*JAK2V617F* cells, combination of 750nM bem and 100nM ruxo is shown (B). Isobologram analysis was performed to test for combination effects of bem and ruxo, combination indices (CI) were calculated based on "Loewe Additivity." CI 0.8–1.2 indicate additivity (C and D). Analysis of downstream pathways after incubation of SET-2 (E) and BaF3-EpoR-*JAK2V617F* (F) cells with the combination of bem (2 μM) and ruxo (50nM) for 1h in serum-deprived conditions was performed by western blot (E and F). CI = combination index; pAKT = phosphorylated AKT; pERK = phosphorylated ERK; pSTAT = phosphorylated STAT; WST-1 = water soluble tetrazolium salts.

Investigation of signal transduction pathways promoting MPN cell growth and survival, revealed that pathways affected by AXL blockade differed between human and murine cells. Pronounced reduction of phosphorylated STAT5 was found in human SET-2 cells, with some inter-experimental variance of inhibition magnitude at lower drug concentrations. In murine cells, phosphorylated AKT levels were significantly decreased upon AXL blockade. In combination with ruxolitinib, bemcentinib treatment exerted additive effects on inhibition of STAT5 and STAT3 signaling in SET-2 cells and of AKT signaling in murine cells, resulting in additive inhibitory effects on viability observed after combined AXL and JAK2 blockade in vitro. Although pathways differed between cell lines, all regulated pathways are known to result in AXL-mediated proliferation and survival.[5] Thus, AXL inhibition induces cell-type dependent and -independent changes in important pro-proliferative and -survival pathways in MPN cells. The reason for cell-type dependent modulations of signaling pathways upon bemcentinib treatment are most likely due to heterogeneity between the cell lines. SET-2 cells represent a megacaryoblastic cell line. BaF3-EpoR-*JAK2V617F* cells are of murine origin and contain the erythropoietin receptor and are therefore most likely more similar to an erythroleukemia cell line. While this reflects the heterogeneity of MPN, further work is necessary to dissect the effects of bemcentinib in different MPN cell types.

The therapeutic effects of AXL inhibition were confirmed in vivo in 2 different models of *JAK2V617F* driven disease, a subcutaneous xenograft and a systemic model of acute MPN disease. Representing a key finding, in vivo studies showed prolonged overall survival and reduced splenomegaly for the combination of bemcentinib and ruxolitinib compared with single

drug treatment, supporting the finding that AXL inhibition exerted additive effects to ruxolitinib inhibition.

Furthermore, our data indicate that bemcentinib is active in primary MPN cells. Importantly, the less pronounced effect of bemcentinib on colony growth of cells from healthy donors compared with patient cells suggests a therapeutic window for the drug. The experience from phase II clinical trials using bemcentinib support the existence of a therapeutic window by showing good drug tolerability.[37] In line with our data, Pearson et al[27] demonstrated that bemcentinib reduced the clonogenic activity of CD34+ cells isolated from JAK2 mutated patients. Different to our in vitro and in vivo data, they did not find an additive effect of bemcentinib and ruxolitinib on the clonogenic activity of primary MPN cells, likely due to the different nature of the performed experiments. Further studies are warranted to investigate whether additivity of the tested drugs translates to the clinic.

During ruxolitinib treatment, cytopenias are common, frequently requiring dose adjustments. Because cytopenias are rarely observed with bemcentinib, the combination of the 2 drugs may increase disease response while allowing treatment with lower doses of ruxolitinib with better tolerability. Beyond that, bemcentinib showed to positively impact erythropoiesis and alleviate anemia in vivo.

Many efforts have been made to identify effective combination partners for ruxolitinib-based treatment. Several ruxolitinib-based combinations have entered clinical trials. However, despite promising preclinical results, so far, most combinations have failed to show convincing clinical efficacy superior to that of ruxolitinib alone.[36,38-41] Our study presents a new approach with the potential to increase disease control and overcome
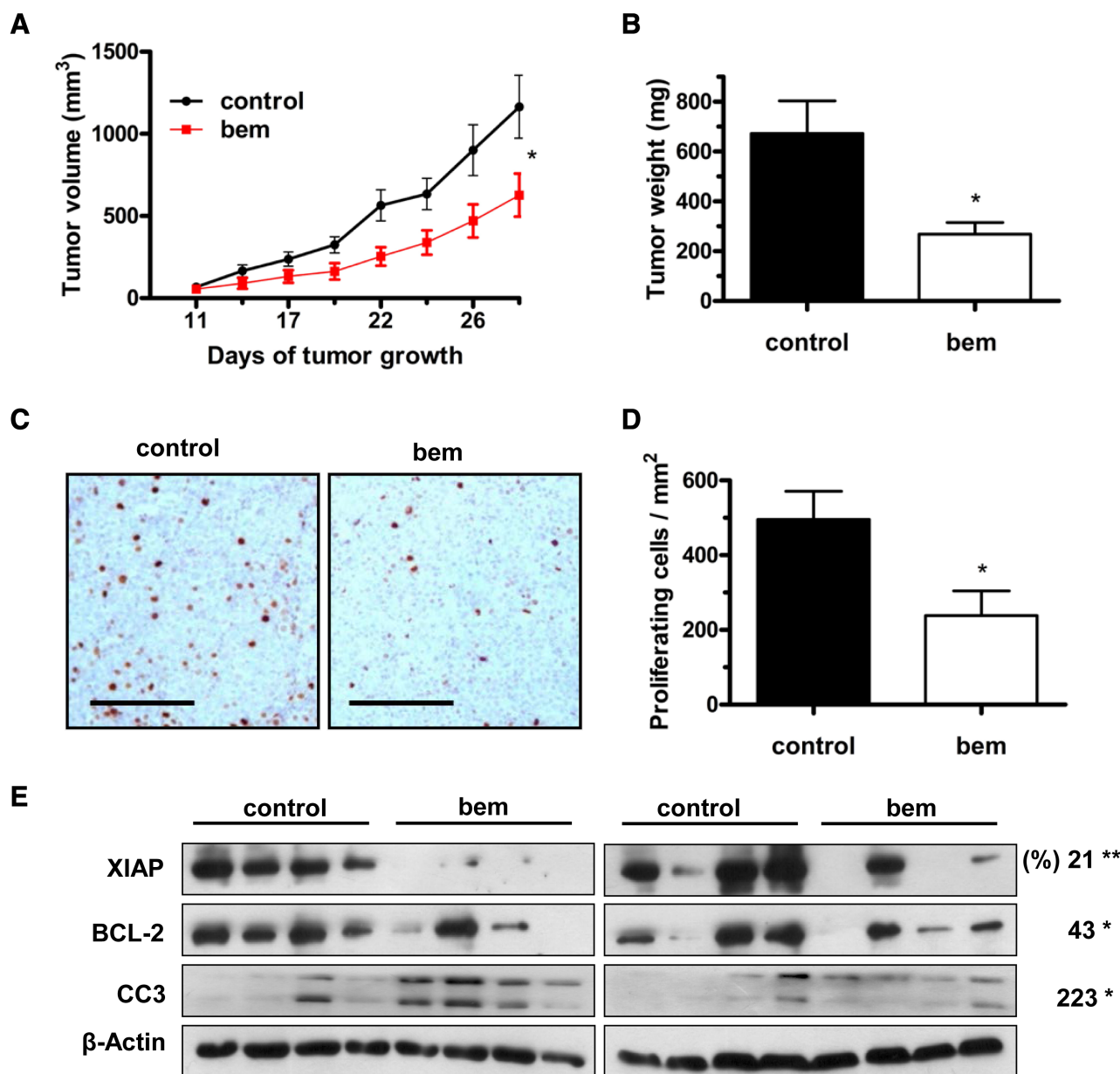
Figure 7. AXL blockade exerts inhibitory effects in vivo. SET-2 cells were injected subcutaneously into the flank of NSG mice followed by randomization and treatment with vehicle or bemcentinib (bem, 50 mg/kg) twice daily (n = 8/8). Tumor growth curves (*$P < 0.05$, 2-way ANOVA) (A) and final tumor weight were compared (n = 8/8, *$P < 0.05$, Student's t test) (B). Representative immunohistochemistry images of phospho-histone H3 stainings on sections from SET-2 control- and bem-treated tumors. Bar represents 50 μm (C). Morphometric analysis of phospho-histone H3+ cells was performed to quantify proliferation of MPN cells in vivo in control- and bem-treated tissues (D). Immunoblots of apoptosis markers XIAP, BCL-2, and CC3 were performed in bem-treated SET-2 tumors (50 mg/kg) compared with control-treated. Densitometric quantification of (protein expression/β-Actin expression) was normalized to control-treated tumors and represented as percentage (n = 8/8, *$P < 0.05$, **$P < 0.01$) (E). CC3 = cleaved caspase 3; MPN = myeloproliferative neoplasm; NSG = nonobese diabetic severe combined immunodeficiency gamma.

resistance in ruxolitinib-treated patients with the clinically applicable AXL inhibitor bemcentinib.

Why could AXL inhibition be useful to enhance efficacy of ruxolitinib? In our study, treatment with ruxolitinib increased activation of AXL as shown by augmented phosphorylation levels. Thus, we demonstrate for the first time that activation of AXL during ruxolitinib treatment could mediate resistance against JAK2 inhibition and thereby decrease efficacy of ruxolitinib treatment in MPN. Consistently, we detected an additive effect of bemcentinib and ruxolitinib in vivo. These data are in line with findings reported in AML and other cancers including melanoma and NSCLC in which AXL upregulation mediated resistance upon treatment with fms-like tyrosine kinase

3 (FLT3), B-raf proto-oncogene serine/threonine-protein, and EGFR inhibitors, respectively.[9,15,16] Preclinical data demonstrate that AXL inhibition with bemcentinib can overcome acquired resistance towards targeted agents and chemotherapy in different disease models.[7,8,18,19] Clinical trials investigating the effectiveness of the combination of bemcentinib and targeted therapies in cancer patients are currently ongoing (NCT03184571, NCT02872259, NCT02424617, NCT03654833).[17,21,26]

Interestingly, we observed increased phosphorylation of AXL after treatment with ruxolitinib that causes hyperphosphorylation of JAK2 and inversely, slightly decreased phosphorylation of AXL after CHZ868 treatment that inhibits JAK2 phosphorylation.[42] Also, co-immunoprecipitation indicated that JAK2
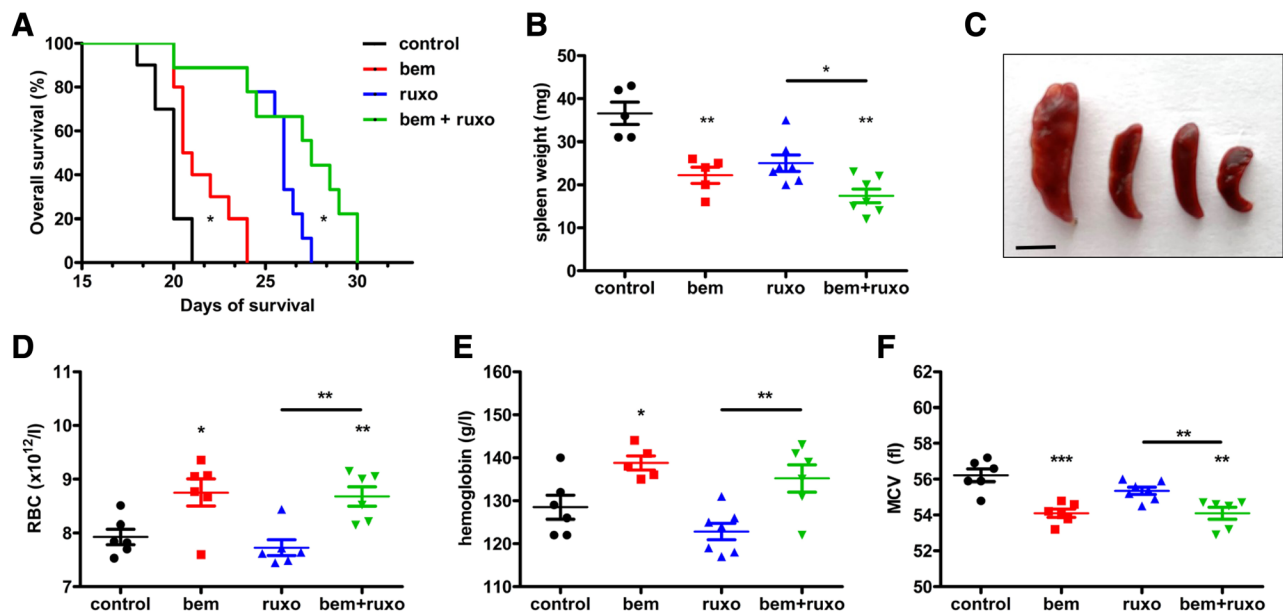
Figure 8. Bemcentinib (bem) and ruxolitinib (ruxo) exert additive effects in vivo. In a systemic model of *JAK2V617F*-driven disease, mice were treated with vehicle, bem (50 mg/kg), ruxo (50 mg/kg), or bem and ruxo (50 mg/kg each) twice daily. For survival analysis mice were sacrificed at first signs of disease, survival analysis was carried out using the Kaplan-Meier method (log-rank test, n = 11/10/10/10) (A). Another cohort of mice was sacrificed on day 18 for phenotyping purposes (n = 6/6/7/7). Spleens were weighed (B), representative spleens from control, bem-, ruxo-, and bem + ruxo-treated mice (from left to right) are displayed (bar represents 5 mm) (C). Blood count analysis was performed and RBC count, hemoglobin levels, and MCV of erythrocytes are shown (D–F, respectively). Significant outliers were identified using Grubb's test and excluded from analysis. Student´s t-test was performed for analysis of statistical difference (*$P < 0.05$, **$P < 0.01$). MCV = mean cellular volume; RBC = red blood cell.

and AXL interact physically. This novel finding corroborates the importance of AXL in JAK2-driven disease.

In FLT3-internal tandem duplication AML, enhanced STAT5 expression represents a bypass mechanism inducing increased AXL expression and resistance towards FLT3-directed targeted therapy.[9] STAT5 plays a major role in hematopoiesis and constitutive STAT5 expression is a key event in the pathogenesis of MPN. Multiple receptors signal through STAT5 in hematopoietic cells, including MERTK.[43] Nothing is known about the emergence of resistance towards AXL inhibition in MPN and the potential role of MERTK to substitute for AXL signaling is unknown in this disease. However, increased MERTK expression after treatment of different solid tumor cell lines with an AXL inhibitor was previously described and overexpression of MERTK resulted in resistance towards AXL inhibition.[44] The potential role of MERTK in mediating resistance to AXL inhibition and other potential resistance mechanisms including enhanced STAT3/5 expression are subject to future studies.

The in vivo models used in our study represent acute models of *JAK2V617F* driven disease.[29,34] Despite the aggressive systemic BaF3-EpoR-*JAK2V617F* model with mean overall survival of merely 20 days in the control group, significant survival advantages and reduction of splenomegaly were achieved with bemcentinib. Moreover, combination treatment with bemcentinib and ruxolitinib showed additive effects on survival and splenomegaly. Interestingly, bemcentinib treatment resulted in increased levels of RBC and hemoglobin in vivo. This positive effect on erythropoiesis was observed after bemcentinib monotherapy and combination therapy but not in ruxolitinib-only treated mice, indicating that reduced BM infiltration alone does not explain this finding. Furthermore, reduced MCV levels in bemcentinib-treated mice compared with MCV levels above the physiologic norm in vehicle-treated mice indicate a normalization of erythropoiesis through AXL inhibition. A role of GAS6-AXL signaling in erythropoiesis was previously described. Erythropoietin receptor signaling in murine erythroblasts was shown to be partly dependent on GAS6, GAS6

treatment in anemic mice resulted in restoration of hematocrit and the erythropoietic response of GAS6 was described to be mediated mainly by AXL while MERTK and TYRO3 signaling did not compensate for the absence of AXL.[45] In Tet methylcytosine dioxygenase 2 deficiency that causes ineffective erythropoiesis AXL upregulation on erythroblasts was observed and AXL inhibition rescued defective erythropoiesis in this context.[46] Altogether, these data indicate that AXL inhibition can positively impact altered erythropoiesis in MPN. Interestingly, pharmacologic blockade of AXL has also been previously described to induce differentiation of megakaryocytes.[47] Nevertheless, subcutaneous models and models in immunocompromised mice have their limitations regarding the study of neoplasms originating in the BM and further studies using more sophisticated models of MPN are warranted in the future.[48,49]

These data form the preclinical rationale for clinical trials of bemcentinib in combination with ruxolitinib as first line treatment in MPN. Furthermore, the clinical evaluation of efficacy of bemcentinib monotherapy in ruxolitinib-refractory disease is warranted.

Our previous work showed GAS6 to be upregulated by mesenchymal cells upon interaction with AML cells in the BM microenvironment.[8] In this study, we found significant higher GAS6 levels in BM plasma of MPN patients in comparison to healthy individuals suggesting that there might be a similar interaction of MPN cells with mesenchymal stem cells resulting in induction of GAS6 secretion by stromal cells. Our study confirms previous findings[27] that levels of GAS6 in PB plasma are not increased in the whole cohort of MPN patients. However, we found that PB GAS6 levels were increased in the subgroup of MF patients only. Altogether, these data indicate that GAS6-AXL signaling might be generally relevant in the BM of MPN patients as opposed to PB. Further studies are needed to prove the source of GAS6 in BM stroma and elucidate the role of GAS6 in MPN.

In summary, our data highlight AXL inhibition as a new therapeutic approach in MPN and support the need for clinical trials of bemcentinib.

Acknowledgments

Disclosures

Sources of funding

References

1. Passamonti F, Maffioli M. Update from the latest WHO classification of MPNs: a user's manual. *Hematology Am Soc Hematol Educ Program*. 2016;2016:534–542.
2. Harrison C, Kiladjian JJ, Al-Ali HK, et al. JAK inhibition with ruxolitinib versus best available therapy for myelofibrosis. *N Engl J Med*. 2012;366:787–798.
3. Pardanani A, Harrison C, Cortes JE, et al. Safety and efficacy of fedratinib in patients with primary or secondary myelofibrosis: a randomized clinical trial. *JAMA Oncol*. 2015;1:643–651.
4. Vannucchi AM, Kiladjian JJ, Griesshammer M, et al. Ruxolitinib versus standard therapy for the treatment of polycythemia vera. *N Engl J Med*. 2015;372:426–435.
5. Linger RM, Keating AK, Earp HS, et al. TAM receptor tyrosine kinases: biologic functions, signaling, and potential therapeutic targeting in human cancer. *Adv Cancer Res*. 2008;100:35–83.
6. Rochlitz C, Lohri A, Bacchi M, et al. Axl expression is associated with adverse prognosis and with expression of Bcl-2 and CD34 in de novo acute myeloid leukemia (AML): results from a multicenter trial of the Swiss Group for Clinical Cancer Research (SAKK). *Leukemia*. 1999;13:1352–1358.
7. Ben-Batalla I, Erdmann R, Jørgensen H, et al. Axl blockade by BGB324 inhibits BCR-ABL tyrosine kinase inhibitor-sensitive and -resistant chronic myeloid leukemia. *Clin Cancer Res*. 2017;23:2289–2300.
8. Ben-Batalla I, Schultze A, Wroblewski M, et al. Axl, a prognostic and therapeutic target in acute myeloid leukemia mediates paracrine crosstalk of leukemia cells with bone marrow stroma. *Blood*. 2013;122:2443–2452.
9. Dumas PY, Naudin C, Martin-Lannerée S, et al. Hematopoietic niche drives FLT3-ITD acute myeloid leukemia resistance to quizartinib via STAT5-and hypoxia-dependent upregulation of AXL. *Haematologica*. 2019;104:2017–2027.
10. Meyer AS, Miller MA, Gertler FB, et al. The receptor AXL diversifies EGFR signaling and limits the response to EGFR-targeted inhibitors in triple-negative breast cancer cells. *Sci Signal*. 2013;6:ra66.
11. Goyette MA, Duhamel S, Aubert L, et al. The receptor tyrosine kinase AXL Is required at multiple steps of the metastatic cascade during HER2-positive breast cancer progression. *Cell Rep*. 2018;23:1476–1490.
12. Ruan GX, Kazlauskas A. Axl is essential for VEGF-A-dependent activation of PI3K/Akt. *EMBO J*. 2012;31:1692–1703.
13. Ghosh AK, Secreto C, Boysen J, et al. The novel receptor tyrosine kinase Axl is constitutively active in B-cell chronic lymphocytic leukemia and acts as a docking site of nonreceptor kinases: implications for therapy. *Blood*. 2011;117:1928–1937.
14. Loges S, Heuser M, Chromik J, et al. Final analysis of the dose escalation, expansion and biomarker correlations in the Ph I/II trial BGBC003 with the selective oral AXL inhibitor bemcentinib (BGB324) in relapsed/refractory AML and MDS. *Blood*. 2018;132(suppl 1):2672–2672.
15. Zhang Z, Lee JC, Lin L, et al. Activation of the AXL kinase causes resistance to EGFR-targeted therapy in lung cancer. *Nat Genet*. 2012;44:852–860.
16. Müller J, Krijgsman O, Tsoi J, et al. Low MITF/AXL ratio predicts early resistance to multiple targeted drugs in melanoma. *Nat Commun*. 2014;5:5712.
17. Hugo W, Zaretsky JM, Sun L, et al. Genomic and transcriptomic features of response to anti-PD-1 therapy in metastatic melanoma. *Cell*. 2016;165:35–44.
18. Wu F, Li J, Jang C, et al. The role of Axl in drug resistance and epithelial-to-mesenchymal transition of non-small cell lung carcinoma. *Int J Clin Exp Pathol*. 2014;7:6653–6661.
19. Sensi M, Catani M, Castellano G, et al. Human cutaneous melanomas lacking MITF and melanocyte differentiation antigens express a functional Axl receptor kinase. *J Invest Dermatol*. 2011;131:2448–2457.
20. Boshuizen J, Koopman LA, Krijgsman O, et al. Cooperative targeting of melanoma heterogeneity with an AXL antibody-drug conjugate and BRAF/MEK inhibitors. *Nat Med*. 2018;24:203–212.
21. Ludwig KF, Du W, Sorrelle NB, et al. Small-molecule inhibition of axl targets tumor immune suppression and enhances chemotherapy in pancreatic cancer. *Cancer Res*. 2018;78:246–255.
22. Taniguchi H, Yamada T, Wang R, et al. AXL confers intrinsic resistance to osimertinib and advances the emergence of tolerant cells. *Nat Commun*. 2019;10:259.
23. Zhou L, Liu XD, Sun M, et al. Targeting MET and AXL overcomes resistance to sunitinib therapy in renal cell carcinoma. *Oncogene*. 2016;35:2687–2697.
24. Lorens J, Arce-Lara CE, Arriola E, et al. Phase II open-label, multi-centre study of bemcentinib (BGB324), a first-in-class selective Axl inhibitor, in combination with pembrolizumab in patients with advanced NSCLC. *J Clin Oncol*. 2018;36(suppl; abstr 3078):2018.
25. Yule M, Davidsen K, Bloe M, et al. Combination of bemcentinib (BGB324): a first-in-class selective oral AXL inhibitor, with pembrolizumab in patients with triple negative breast cancer and adenocarcinoma of the lung. *J Clin Oncol*. 2018;36(5_suppl):TPS43–TPS43.
26. Straume O, Schuster C, Gausdal G, Lorens J, Gjertsen BT. A randomized phase Ib/II study of the selective small molecule axl inhibitor bemcentinib (BGB324) in combination with either dabrafenib/trametinib or pembrolizumab in patients with metastatic melanoma. *J Clin Oncol*. 2018;36(15_suppl):9548–9548.
27. Pearson S, Blance R, Somervaille TCP, et al. AXL inhibition extinguishes primitive JAK2 mutated myeloproliferative neoplasm progenitor cells. *HemaSphere*. 2019;3:e233.
28. Weber K, Bartsch U, Stocking C, et al. A multicolor panel of novel lentiviral "gene ontology" (LeGO) vectors for functional gene analysis. *Mol Ther*. 2008;16:698–706.
29. Quintás-Cardama A, Vaddi K, Liu P, et al. Preclinical characterization of the selective JAK1/2 inhibitor INCB018424: therapeutic implications for the treatment of myeloproliferative neoplasms. *Blood*. 2010;115:3109–3117.
30. Loges S, Batalla IB, Heuser M, et al. Axl blockade in vitro and in patients with high-risk MDS by the small molecule inhibitor BGB324. *J Clin Oncol*. 2017;35(15_suppl):7059–7059.
31. Deveraux QL, Takahashi R, Salvesen GS, et al. X-linked IAP is a direct inhibitor of cell-death proteases. *Nature*. 1997;388:300–304.
32. Vaux DL, Cory S, Adams JM. Bcl-2 gene promotes haemopoietic cell survival and cooperates with c-myc to immortalize pre-B cells. *Nature*. 1988;335:440–442.
33. Porter AG, Jänicke RU. Emerging roles of caspase-3 in apoptosis. *Cell Death Differ*. 1999;6:99–104.

34. Hart S, Goh KC, Novotny-Diermayr V, et al. SB1518, a novel macrocyclic pyrimidine-based JAK2 inhibitor for the treatment of myeloid and lymphoid malignancies. *Leukemia*. 2011;25:1751–1759.

35. Knibbe-Hollinger JS, Fields NR, Chaudoin TR, et al. Influence of age, irradiation and humanization on NSG mouse phenotypes. *Biol Open*. 2015;4:1243–1252.

36. Pardanani A, Tefferi A. How I treat myelofibrosis after failure of JAK inhibitors. *Blood*. 2018;132:492–500.

37. Loges S, Gjertsen B-T, Heuser M, et al. The immunomodulatory activity of bemcentinib (BGB324) - a first-in-class selective, oral AXL inhibitor in patients with relapsed/refractory acute myeloid leukemia or myelodisplastic syndrome. Paper presented at: ASCO-SITC Clinical Immuno-Oncology Symposium;June 1–5, 2018; San Francisco, CA.

38. Couban S, Benevolo G, Donnellan W, et al. A phase Ib study to assess the efficacy and safety of vismodegib in combination with ruxolitinib in patients with intermediate- or high-risk myelofibrosis. *J Hematol Oncol*. 2018;11:122.

39. Gowin K, Kosiorek H, Dueck A, et al. Multicenter phase 2 study of combination therapy with ruxolitinib and danazol in patients with myelofibrosis. *Leuk Res*. 2017;60:31–35.

40. Daver N, Cortes J, Newberry K, et al. Ruxolitinib in combination with lenalidomide as therapy for patients with myelofibrosis. *Haematologica*. 2015;100:1058–1063.

41. Masarova L, Verstovsek S, Hidalgo-Lopez JE, et al. A phase 2 study of ruxolitinib in combination with azacitidine in patients with myelofibrosis. *Blood*. 2018;132:1664–1674.

42. Meyer SC, Keller MD, Chiu S, et al. CHZ868, a type II JAK2 inhibitor, reverses type I JAK inhibitor persistence and demonstrates efficacy in myeloproliferative neoplasms. *Cancer Cell*. 2015;28:15–28.

43. Brandao LN, Winges A, Christoph S, et al. Inhibition of MerTK increases chemosensitivity and decreases oncogenic potential in T-cell acute lymphoblastic leukemia. *Blood Cancer J*. 2013;3:e101.

44. McDaniel NK, Cummings CT, Iida M, et al. MERTK mediates intrinsic and adaptive resistance to AXL-targeting agents. *Mol Cancer Ther*. 2018;17:2297–2308.

45. Angelillo-Scherrer A, Burnier L, Lambrechts D, et al. Role of Gas6 in erythropoiesis and anemia in mice. *J Clin Invest*. 2008;118:583–596.

46. Qu X, Zhang S, Wang S, et al. TET2 deficiency leads to stem cell factor-dependent clonal expansion of dysfunctional erythroid progenitors. *Blood*. 2018;132:2406–2417.

47. Suknuntha K, Choi YJ, Jung HS, et al. Megakaryocytic expansion in gilteritinib-treated acute myeloid leukemia patients is associated with AXL inhibition. *Front Oncol*. 2020;10:585151.

48. Lanikova L, Babosova O, Prchal JT. Experimental modeling of myeloproliferative neoplasms. *Genes (Basel)*. 2019;10:E813.

49. Jacquelin S, Kramer F, Mullally A, et al. Murine models of myelofibrosis. *Cancers (Basel)*. 2020;12:E2381.